PERGAMON

International Journal of Solids and Structures 40 (2003) 7055–7062

INTERNATIONAL JOURNAL OF SOLIDS and STRUCTURES

www.elsevier.com/locate/ijsolstr

Failure plane orientations for transverse loading of a unidirectional fiber composite ☆

Richard M. Christensen [a,b,*], Steven J. DeTeresa [a]

[a] *Lawrence Livermore National Laboratory, University of California, Livermore, CA 94550, USA*
[b] *Stanford University, Stanford, CA 94305, USA*

Received 18 September 2002

Dedicated to Professor George J. Dvorak in recognition of his fundamental research contributions to the mechanics of materials and his highly valued service to the profession

Abstract

Using a recently developed failure theory for transversely isotropic fiber composites, it is shown how the orientation of the failure surface can be determined for transverse tension and compression. It is also shown that failure surface orientations decompose into those of ductile type versus those of brittle type. Experimental data on failure surface orientations have been obtained for carbon fiber composite systems based on both thermoplastic and thermosetting matrix materials. Average compression failure planes for the different composite materials were measured to range from 31° to 38° from the load axis. Reasonable agreement was obtained between these measured angles and those predicted from application of the new failure theory.
Published by Elsevier Ltd.

Keywords: Failure theories; Failure surface prediction; Transverse loading

1. Introduction and failure forms

Failure plane orientations comprise an important piece of information when examining the failure modes of materials. This is true of both isotropic materials and fiber reinforced materials, which are normally taken to be transversely isotropic, as will be done here. For both material types the theoretical basis of relevant failure criteria is a rather controversial topic, with many competing forms. It appears that failure mode types and failure surface orientations could and can be used to discriminate between the various forms. The present work proceeds along one such line.

☆ Work was performed under the auspices of the US Department of Energy by the Lawrence Livermore National Laboratory under contract no. W-7405-Eng-48.

* Corresponding author. Address: Stanford University, Stanford, CA 94305, USA. Tel.: +1-925-422-7136; fax: +1-925-423-2405.
E-mail address: christensen@stanford.edu (R.M. Christensen).

0020-7683/$ - see front matter Published by Elsevier Ltd.
doi:10.1016/S0020-7683(03)00354-8

The particular fiber composite failure criterion to be considered here is the five-parameter form given by Christensen (1998). The failure criterion is partitioned into fiber controlled failure modes and matrix controlled failure modes. First, recalling the matrix controlled form and then the fiber controlled form:

Matrix controlled:

$$\alpha_1 k_1(\sigma_{22}+\sigma_{33})+(1+2\alpha_1)\left[\frac{(\sigma_{22}-\sigma_{33})^2}{4}+\sigma_{23}^2\right]+\beta_1(\sigma_{12}^2+\sigma_{31}^2)\leqslant k_1^2 \tag{1}$$

where

$$\begin{aligned} k_1 &= \frac{|\sigma_{22}^{\mathrm{C}}|}{2} \\ \alpha_1 &= \frac{1}{2}\left(\frac{|\sigma_{22}^{\mathrm{C}}|}{\sigma_{22}^{\mathrm{T}}}-1\right) \\ \beta_1 &= \left(\frac{\sigma_{22}^{\mathrm{C}}}{2\sigma_{12}^{\mathrm{Y}}}\right)^2 \end{aligned} \tag{2}$$

where Cartesian coordinate notation is used with axis 1 in the fiber direction, and three dimensional effects are considered. The five failure properties are the 1-D axial and transverse normal stress failure values and the longitudinal shear failure value: σ_{11}^{T}, σ_{11}^{C}, σ_{22}^{T}, σ_{22}^{C}, σ_{12}^{Y}

Fiber controlled:

$$-\alpha_2 k_2\sigma_{11}+\frac{1}{4}(1+2\alpha_2)\sigma_{11}^2-\frac{(1+\alpha_2)^2}{4}(\sigma_{22}+\sigma_{33})\sigma_{11}\leqslant k_2^2 \tag{3}$$

where

$$\begin{aligned} k_2 &= \frac{\sigma_{11}^{\mathrm{T}}}{2} \\ \alpha_2 &= \frac{1}{2}\left(\frac{\sigma_{11}^{\mathrm{T}}}{|\sigma_{11}^{\mathrm{C}}|}-1\right) \end{aligned} \tag{4}$$

For applicational purposes forms (2) can be inserted in (1) and forms (4) into (3) to give the concise failure forms:

Fiber controlled:

$$\left(\frac{1}{T_{11}}-\frac{1}{C_{11}}\right)\sigma_{11}+\frac{\sigma_{11}^2}{T_{11}C_{11}}-\frac{1}{4}\left(\frac{1}{T_{11}}+\frac{1}{C_{11}}\right)^2(\sigma_{22}+\sigma_{33})\sigma_{11}\leqslant 1 \tag{5}$$

Matrix controlled:

$$\left(\frac{1}{T_{22}}-\frac{1}{C_{22}}\right)(\sigma_{22}+\sigma_{33})+\frac{1}{T_{22}C_{22}}[(\sigma_{22}-\sigma_{33})^2+4\sigma_{23}^2]+\frac{(\sigma_{12}^2+\sigma_{31}^2)}{S_{12}^2}\leqslant 1 \tag{6}$$

where

$$T_{11}=\sigma_{11}^{\mathrm{T}},\quad T_{22}=\sigma_{22}^{\mathrm{T}},\quad C_{11}=|\sigma_{11}^{\mathrm{C}}|,\quad C_{22}=|\sigma_{22}^{\mathrm{C}}|,\quad S_{12}=\sigma_{12}^{\mathrm{Y}} \tag{7}$$

For 2-D plane stress conditions, take the out-of-plane stress components as vanishing

$$\sigma_{33}=\sigma_{31}=\sigma_{23}=0$$

Then from the 3-D fiber controlled criterion (5) gives the reduced 2-D form:

Fiber controlled:

$$\left(\frac{1}{T_{11}}-\frac{1}{C_{11}}\right)\sigma_{11}+\frac{\sigma_{11}^2}{T_{11}C_{11}}-\frac{1}{4}\left(\frac{1}{T_{11}}+\frac{1}{C_{11}}\right)^2\sigma_{11}\sigma_{22}\leqslant 1 \tag{8}$$

In the plane stress condition (but not necessarily in the 3-D case) it is common to have the transverse normal stress very small compared with the axial normal stress, $\sigma_{22}\ll\sigma_{11}$. In this case, (8) becomes the usual maximum stress criterion

$$-C_{11}\leqslant\sigma_{11}\leqslant T_{11} \tag{9}$$

Still in the plane stress condition, the 3-D form (6) becomes the 2-D form:

Matrix controlled:

$$\left(\frac{1}{T_{22}}-\frac{1}{C_{22}}\right)\sigma_{22}+\frac{\sigma_{22}^2}{T_{22}C_{22}}+\frac{\sigma_{12}^2}{S_{12}^2}\leqslant 1 \tag{10}$$

Forms (5) and (6) for 3-D conditions and (8) or (9) with (10) for 2-D plane stress conditions are among the very simplest forms for fiber composite failure criteria which have a theoretical and physical basis.

The specific failure orientation problem of interest here is that of the failure surface for matrix controlled failure under transverse stress σ_{22}, both in tensile and compressive states. In this case it will be advantageous to use the forms (1) and (2) rather than the simpler forms just given which would be the best forms for design applications. The present approach and the approach taken by Puck and Schürmann (1998) based upon the Coulomb–Mohr method for isotropic materials appear to be the only fiber composite failure forms which have been investigated in this failure surface orientation context. It is quite interesting to pursue these failure mode characteristics because it provides a useful evaluation tool, not only in comparing various theories, but also in assessing failure mode types as being of brittle or ductile characteristics.

2. Failure plane orientations

In considering the possible orientations of the failure planes for fiber composites under transverse tension and compression, it is necessary here to start with appropriate failure criteria. Under transverse stress conditions, the failure characteristics are what are usually designated as matrix controlled or dominated, as opposed to fiber controlled, the latter of which relate to stress in the fiber direction. Fiber composite failure criteria have been recently derived by Christensen (1998) allowing a decomposition into both modes of possible failure behavior at the lamina level. Only the matrix controlled criterion is needed here and from (1) with the longitudinal shear stress taken as vanishing

$$\alpha_1 k_1(\sigma_{22}+\sigma_{33})+(1+2\alpha_1)\left[\frac{(\sigma_{22}-\sigma_{33})^2}{4}+\sigma_{23}^2\right]\leqslant k_1^2 \tag{11}$$

where α_1 and k_1 are given by (2).

The transverse stresses at failure from (11) and (2) are given by

$$\sigma_{22}^{\mathrm{T}}=\frac{2k_1}{1+2\alpha_1}$$
$$\sigma_{22}^{\mathrm{C}}=-2k_1 \tag{12}$$

The associated flow rule will be taken as governing the nonlinear increments of "plastic" strain at failure, i.e.,

$$\dot{\varepsilon}_{ij}^{\mathrm{p}}=\lambda\frac{\partial f}{\partial\sigma_{ij}} \tag{13}$$

where (11) at failure is written as

$$f(\sigma_{ij}) = k_1^2 \tag{14}$$

Using (13) with $f(\ )$ from (11) gives the increments of plastic strain as

$$\begin{aligned}
&\dot{\varepsilon}^{\mathrm{p}}_{11} = 0 \\
&\frac{\dot{\varepsilon}^{\mathrm{p}}_{22}}{\lambda} = \alpha_1 k_1 + \frac{(1+2\alpha_1)}{2}(\sigma_{22} - \sigma_{33}) \\
&\frac{\dot{\varepsilon}^{\mathrm{p}}_{33}}{\lambda} = \alpha_1 k_1 + \frac{(1+2\alpha_1)}{2}(\sigma_{33} - \sigma_{22}) \\
&\frac{\dot{\varepsilon}^{\mathrm{p}}_{23}}{\lambda} = 2(1+2\alpha_1)\sigma_{23} \\
&\frac{\dot{\varepsilon}^{\mathrm{p}}_{12}}{\lambda} = \frac{\dot{\varepsilon}^{\mathrm{p}}_{31}}{\lambda} = 0
\end{aligned} \tag{15}$$

where λ in (13) and (15) is a scalar factor.

From this point onward, consider only the case of the single transverse normal stress

$$\sigma_{22} \neq 0 \quad \text{other} \quad \sigma_{ij} = 0 \tag{16}$$

Then all strain increments vanish except $\dot{\varepsilon}^{\mathrm{p}}_{22}$ and $\dot{\varepsilon}^{\mathrm{p}}_{33}$ in (15), repeated here as

$$\begin{aligned}
&\frac{\dot{\varepsilon}^{\mathrm{p}}_{22}}{\lambda} = \alpha_1 k_1 + \frac{(1+2\alpha_1)}{2}\sigma_{22} \\
&\frac{\dot{\varepsilon}^{\mathrm{p}}_{33}}{\lambda} = \alpha_1 k_1 - \frac{(1+2\alpha_1)}{2}\sigma_{22}
\end{aligned} \tag{17}$$

Using the stresses at failure (12) in (17) gives for

Compression:

$$\begin{aligned}
&\frac{\dot{\varepsilon}^{\mathrm{p}}_{22}}{\lambda k_1} = -1 - \alpha_1 \\
&\frac{\dot{\varepsilon}^{\mathrm{p}}_{33}}{\lambda k_1} = 1 + 3\alpha_1
\end{aligned} \tag{18}$$

and for

Tension:

$$\begin{aligned}
&\frac{\dot{\varepsilon}^{\mathrm{p}}_{22}}{\lambda k_1} = 1 + \alpha_1 \\
&\frac{\dot{\varepsilon}^{\mathrm{p}}_{33}}{\lambda k_1} = -1 + \alpha_1
\end{aligned} \tag{19}$$

Next we introduce the key hypothesis that permits the determination of the failure plane direction. Take the failure surface orientation such that the normal strain increment in the plane of the failure surface either vanishes, or if that is not possible, is a minimum, while the other two strain increments—shear and normal strain normal to the surface—lead to unbounded strains in the failure process, symptomatic of rupture.

First consider the case of transverse compressive stress. Take a Mohr's circle representation for the strain increments $\dot{\varepsilon}^{\mathrm{p}}_{22}$, $\dot{\varepsilon}^{\mathrm{p}}_{33}$ (18), and $\dot{\varepsilon}^{\mathrm{p}}_{23}$ (Fig. 1). Following the above stated failure plane orientation hypothesis, angle θ in Fig. 1 is the angle from direction 2, the loading axis, to the failure plane having a vanishing

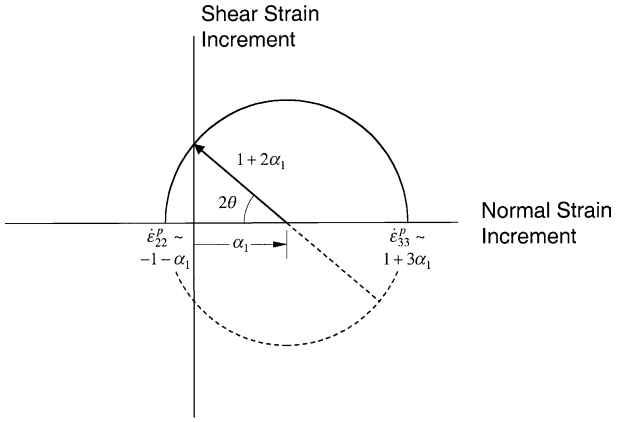

Fig. 1. Determination of transverse compression failure plane orientation.

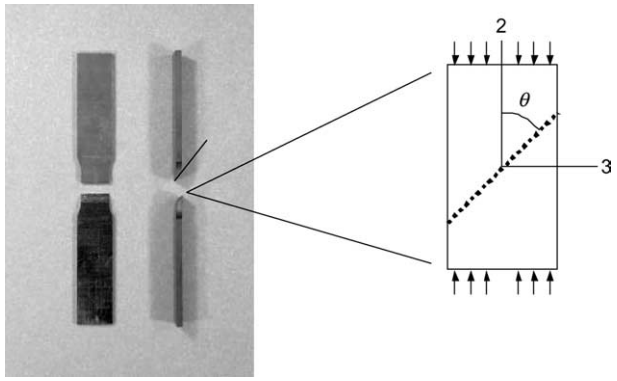

Fig. 2. Orientation of failure plane.

normal strain increment in the plane of the failure surface. This orientation is as shown in Fig. 2. From Fig. 1, failure angle θ is given by

$$\theta_{\mathrm{COMP}} = \frac{1}{2}\cos^{-1}\left(\frac{\alpha_1}{1+2\alpha_1}\right) \tag{20}$$

Now consider the transverse tension case. The strain increments are given by (19) (Fig. 3). The failure plane angle θ is given by

$$\begin{aligned} &\theta_{\mathrm{TEN}} = \frac{1}{2}\cos^{-1}(-\alpha_1), \quad \alpha_1 \leqslant 1 \\ &\theta_{\mathrm{TEN}} = 90^\circ, \quad \alpha_1 \geqslant 1 \end{aligned} \tag{21}$$

For $\alpha_1 \leqslant 1$ the normal strain increment in the plane of the failure vanishes, as seen in Fig 3. However, when $\alpha_1 > 1$ then the strain increment in the failure plane is given by $\dot{\varepsilon}^{\mathrm{p}}_{33}$ which is a minimum, but does not vanish.

These results from (20) and (21) are as shown in Fig. 4. The orientational characteristics of the failure plane are seen to change quite drastically at $\alpha_1 = 1$. From (2) it is seen that

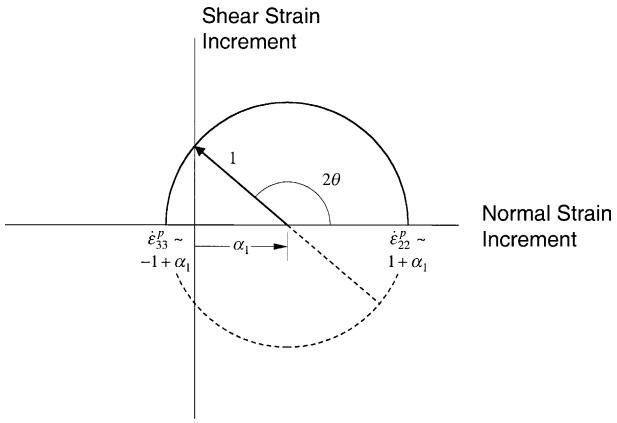

Fig. 3. Determination of transverse tensile failure plane orientation.

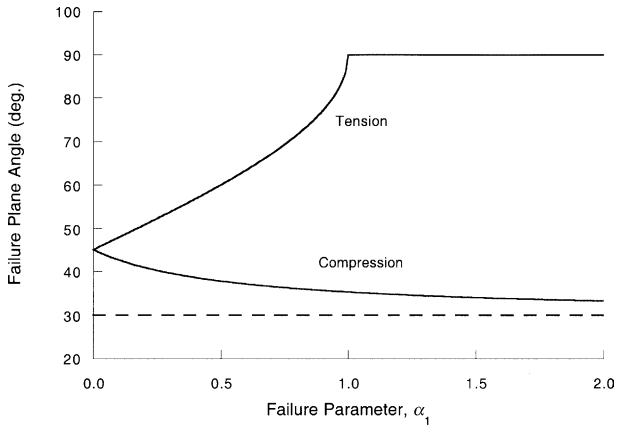

Fig. 4. Predicted orientation of failure planes in tension and compression.

$$\frac{\sigma_{22}^{\mathrm{T}}}{|\sigma_{22}^{\mathrm{C}}|} = \frac{1}{3} \quad \text{at } \alpha_1 = 1 \tag{22}$$

This value of $\sigma_{22}^{\mathrm{T}}/|\sigma_{22}^{\mathrm{C}}|$ is very close to the values commonly reported for graphite fiber-polymer matrix composites. Thus, according to (21) and Fig. 4 such composites are right at the threshold of brittle behavior as characterized by a failure surface which is normal to the loading direction when in tension. Two other characteristics are also of importance. At $\alpha_1 = 0$, where the tensile and compressive failure stresses are of the same magnitudes, the failure angles from both (20) and (21) are given by $\theta = \pm 45°$. This is the common failure angle associated with ductile failure under maximum shear stress. At the other extreme, $\alpha_1 \to \infty$, corresponding to a very damaged material with negligible tensile failure stress, the failure angle θ for compression (20), approaches an asymptote of 30°. As suggested by the Fig. 4 results, in uniaxial tension $\alpha_1 < 1$ gives ductile failure and $\alpha_1 > 1$ gives brittle failure. In uniaxial compression the failure is always of the ductile type.

For heavily damaged materials with $\alpha_1 \gg 1$, relations (19) show that under uniaxial tension the material tends to expand uniformly. That is, the nonlinear plastic strain increments are positive in the transverse

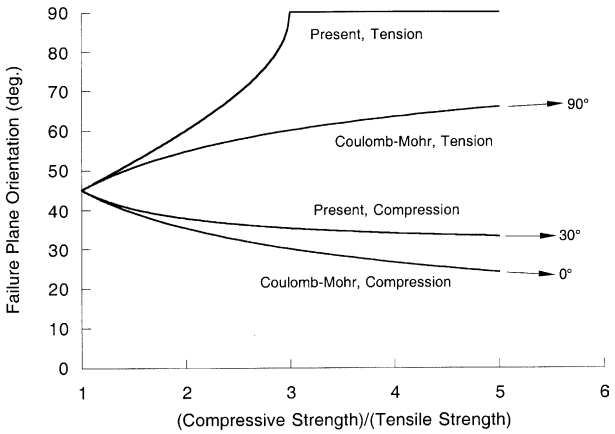

Fig. 5. Comparison of failure plane predictions of present theory with the Coulomb–Mohr theory.

direction and are almost as large as those in the direction of the applied stress. The material is effectively governed by dilatational behavior.

The present failure plane angles are compared with those predicted by the Coulomb–Mohr theory in Fig. 5. The Coulomb–Mohr forms are those derived by Paul (1968) for an isotropic material, appropriate here since the present case of transverse loading is isotropic in the plane. The Coulomb–Mohr results do not show the transition from ductile to brittle behaviors in tension. The failure plane only approaches the fracture-controlled 90° orientation in the limit as the tensile strength becomes negligible compared with the compressive strength. Also, the compressive failure plane angle approaches 0° orientation in the same limit. The Coulomb–Mohr forms do not appear to have a physically realistic behavior.

3. Comparison with experimental results

The predictions of failure plane angles were compared with experimental results for two different carbon fiber composite materials. Both utilized AS4 carbon fiber, but one material had a ductile thermoplastic matrix (Ultem polyetherimide) and the other a relatively brittle matrix (3501-6 untoughened epoxy). Tests were conducted at quasi-static rates using standard rectangular specimens for transverse tensile tests and a tapered-width specimen for compression tests. Only failures that occurred in the gage section were used to determine both the transverse strengths and the orientation of the failure surfaces. A summary of the test results is given in Table 1. The difference in ductility between the two materials is evident in the degree of

Table 1
Experimental results for transverse tension and compression failure

Material	Transverse strengths (ksi)		α_1	Failure plane angles (deg)			
				Tension		Compression	
	Tension	Compression		Predicted	Measured	Predicted	Measured
AS4/Ultem	11.4	27.7	0.71	68	90	36	38(±1.2)[a]
AS4/3501-6	9.4	35.0	1.36	90	90	34	31(±4.7)

[a] Standard deviation.

disparity between the transverse strengths. As measured by the parameter α_1, the two materials are just above and below the threshold of brittle behavior ($\alpha_1 = 1$).

The agreement between experimental results and predictions is reasonable for compression, but all tensile failure planes were oriented at 90° even though the theoretical value is less than this for the more ductile system. It is seen in Fig. 4 that the sensitivity of the tensile failure plane orientation to α_1 is high as it approaches the value one and small experimental errors in the strength values could contribute to the discrepancy. Furthermore, the failure of a typical test coupon is unstable due to the release of significant stored energy in the material and testing equipment. It was thought that a better comparison might be made using crossply laminates to determine the orientation of transverse microcracks, which are generated by a more stable fracture process. However, observations of the orientations of transverse microcracks showed that although some failure planes in the ductile material were oriented at angles less than 90°, in general the planes were closer to 90° than to the predicted value of 68°. Furthermore, many cracks exhibited curvature and branching, which made it difficult to determine an average orientation for the failure plane.

4. Conclusions

A way to discriminate between various forms of failure theories for fiber composites is by determining failure mode types and failure surface orientations. In this paper a prediction for the orientation of failure planes under transverse loading was derived using a recently proposed stress-based failure theory for a fiber composite lamina. In general the agreement with experimental results was good for two carbon fiber composite materials exhibiting significant differences in ductility, especially for the case of transverse compression.

Acknowledgements

The authors gratefully acknowledge the support by the Office of Naval Research, program manager, Dr. Y. Rajapakse. S. DeTeresa is also grateful for the support of the Joint DoD/DOE Advanced Munitions Technology Program, Technical Coordinating Group XII, led by Dr. C. Hoppel of the U.S. Army Research Laboratory. The contributions of Mr. Gregory Larsen to conduct the experiments are greatly appreciated.

References

Christensen, R.M., 1998. The numbers of elastic properties and failure parameters for fiber composites. J. Eng. Mater. Technol. Trans. ASME 120, 110–113.

Paul, B., 1968. Macroscopic criteria for plastic flow and brittle fracture. In: Liebowitz, H. (Ed.), Fracture, vol. II. Academic Press, New York, pp. 313–496.

Puck, A., Schürmann, H., 1998. Failure analysis of FRP laminates by means of physically based phenomenological models. Compos. Sci. Technol. 58, 1045–1067.